

Dynamic Tail Inference with Log-Laplace Volatility

Gordon V. Chavez*

University of California San Francisco

Abstract

We propose a family of stochastic volatility models that enable predictive estimation of time-varying extreme event probabilities in time series with nonlinear dependence and power law tails. The models are a white noise process with conditionally log-Laplace stochastic volatility. In contrast to other, similar stochastic volatility formalisms, this process has an explicit, closed-form expression for its conditional probability density function, which enables straightforward estimation of dynamically changing extreme event probabilities. The process and volatility are conditionally Pareto-tailed, with tail exponent given by the reciprocal of the log-volatility's mean absolute innovation. These models thus can accommodate conditional power law-tail behavior ranging from very weakly non-Gaussian to Cauchy-like tails. Closed-form expressions for the models' conditional polynomial moments also allows for volatility modeling. We provide a computationally straightforward, probabilistic method-of-moments estimation procedure that uses an asymptotic approximation of the process' conditional large deviation probabilities. We demonstrate the estimator's usefulness with a simulation study. We then give an empirical application, which shows that this simple modeling method can be effectively used for dynamic and predictive tail inference in heavy-tailed financial time series.

Keywords: Stochastic volatility, Heavy tails, Extreme events, Nonlinear time series, Tail risk
AMS 2010 Subject Classification: 60G70, 62G32, 62M10, 62P05, 62P12, 91G70

*gordon.chavez@ucsf.edu

1 Introduction

Financial time series data is well-known to exhibit nonlinear dependence and “fat tails”. Such time series often display trends of increasing or decreasing volatility, along with a propensity for extreme values that is far greater than what would be predicted from a Gaussian or other distribution with finite polynomial moments. The latter observation was probably most famously addressed with the early Pareto-tailed and stable models for financial time series proposed by Mandelbrot (1963) and Fama (1968), while the most well-known early approaches to the nonlinear dependence problem were given by Engle (1982) and Bollerslev (1986) with original and generalized autoregressive conditional heteroskedasticity (ARCH, GARCH) models. Since then a great deal of research has been dedicated to extreme event probability estimation and nonlinear time series modeling for financial applications (e.g., Embrechts et. al. 2011 and Terasvirta et. al. 2010).

Estimation of extreme event probabilities is a very important problem for risk and portfolio management. Many estimators for the tail exponent of a marginal distribution have been proposed, e.g., by Hill (1975), Pickands (1975), and deHaan and Resnick (1980), however, these estimators are very sensitive to dependence in the data (Kearns and Pagan 1997, Diebold et. al. 2000). This makes them often ill-suited for application to many strongly dependent time series of interest for financial modeling, i.e., the squares and moduli of financial log-returns (Embrechts et. al. 2011 p. 270, 406). Relatedly, these estimators along with much of extreme value theory (EVT) are designed for inference of stationary, rather than time-varying, tail behavior. Gardes and Girard (2008) and Gardes and Stupfler (2014) have given nonparametric estimators for time-varying tail exponents, while Kelly (2014) has given a parametric approach to dynamic power law estimation in financial time series. The parametric modeling method we propose here, however, does not assume a time-varying tail exponent. Our approach is hence closer to McNeil and Frey’s (2000) combination of stationary EVT with GARCH modeling. However, we use a novel, stochastic volatility approach to enable such dynamic tail inference.

A canonical form of stochastic volatility model, first proposed by Taylor (1982, 1986), is given by

$$\varepsilon_t = \sigma_t z_t, \tag{1.1}$$

where z_t is an *i.i.d.* process with a mean of 0 and a variance of 1, and σ_t is a non-negative process defined by

$$\sigma_t = \exp(H_t), \tag{1.2}$$

where H_t is a Gaussian process with mean μ_H and variance $\sigma_H^2 < \infty$. An important example was the AR(1) model $H_t = \mu_H + \beta(H_{t-1} - \mu_H) + h_t$, where $\beta \in \mathbb{R}$ and $h_t \sim \mathcal{N}(0, \sigma_h^2)$ is *i.i.d.* The kind of model in (1.1) and (1.2), where H_t is a variety of Gaussian processes, has been extensively applied and studied, e.g., to exchange rate modeling by Harvey et. al. (1994) and extended to long-memory Gaussian H_t by Breidt et. al. (1998). However, the stochastic volatility σ_t in (1.2) follows a log-normal distribution, which has finite polynomial moments (see Johnson et. al. 1994). As a consequence, (1.1) also has bounded moments in the usual case of Gaussian z_t . This can be problematic for modeling time series with power law tails and divergent higher-order polynomial moments. Practically, such models will underestimate the probabilities of extreme events. To remedy this, z_t has often been chosen to follow the heavier-tailed Student’s t -distribution, e.g., in Harvey et. al. (1994), Liesenfeld and Jung (2000), and Chib et. al. (2002). However, with a Gaussian or Student’s t choice for z_t and Gaussian H_t , the model (1.1) does not have an explicit, closed-form expression for its conditional distributions. This makes estimation of model parameters as well as outcome probabilities difficult, often requiring the use of Bayesian and Monte Carlo methods such as those described in Jacquier et. al. (1994), Kim et. al. (1998), Sandmann and Koopman (1998),

or Chib et. al. (2002). Reliable estimation of similar, conditionally Student's t-distributed, ARCH-related models requires similar numerical procedures (see, e.g., Mousazadeh and Karimi 2007, Ardia 2008, Ardia and Hoogerheide 2010).

In this paper we propose a stochastic volatility formalism that enables straightforward and computationally inexpensive estimation of time-varying extreme event probabilities in time series with power law tail behavior. The models we present have the form (1.1)-(1.2), with $z_t \sim \mathcal{N}(0, 1)$. However, instead of defining (1.2)'s H_t as Gaussian, we make H_t conditionally *Laplace*-distributed, defining H_t as

$$H_t = E \{H_t | \mathcal{F}_{t-1}\} + h_t, \quad (1.3)$$

where \mathcal{F}_{t-1} is the filtration up to time $t - 1$ and h_t is *i.i.d.* Laplace-distributed with density

$$p_h(h_t) = \frac{1}{2\Delta} \exp\left(-\frac{|h_t|}{\Delta}\right), \quad (1.4)$$

where $\Delta > 0$. This simple but important adjustment endows (1.1)-(1.2)'s σ_t and ε_t with power law-tailed conditional probability density functions, for which there are closed-form expressions. These conditional densities give the result

$$P\{|\varepsilon_t| \geq \Lambda | \mathcal{F}_{t-1}\} \sim f(\Delta) \exp\left(\frac{E\{H_t | \mathcal{F}_{t-1}\}}{\Delta}\right) \Lambda^{-1/\Delta} \quad (1.5)$$

as $\Lambda \rightarrow \infty$. Hence H_t 's mean absolute innovation Δ specifies the tail exponent, which allows (1.1)-(1.4) to flexibly define processes ranging from only mildly non-Gaussian with $\Delta \approx 0$ to processes with Cauchy-like tails at $\Delta = 1$. The process ε_t 's tail probabilities are also strongly and explicitly dependent on the process H_t , which enables their dynamic estimation. We give a simple, probabilistic method-of-moments estimation procedure for the tail exponent, which takes advantage of the result (1.5) for ε_t 's tail probabilities. We present a simulation study to show the effectiveness of the estimator. We then give an empirical application to S&P 500 Index data, which shows that this modeling method can be used for dynamic and predictive estimation of volatility and extreme event probabilities in power law-tailed financial time series. We give some concluding remarks, an appendix with proofs of the main results, and a second appendix, which shows that very similar results, including (1.5), can also be derived for the case when z_t is Laplace-distributed. We lastly give a third appendix with an empirical study of urban air pollution data and solar activity data.

2 Model

We will denote H_t 's conditional expectation as $\bar{H}_t = E\{H_t | \mathcal{F}_{t-1}\}$. We first give expressions for σ_t 's conditional probability density and ε_t 's conditional polynomial moments.

Lemma 2.1. *Given (1.3)-(1.4), σ_t in (1.2) is conditionally distributed according to the log-Laplace probability density function*

$$p_\sigma(\sigma_t | \mathcal{F}_{t-1}) = \begin{cases} \frac{1}{2\Delta} \exp\left(-\frac{\bar{H}_t}{\Delta}\right) \sigma_t^{1/\Delta-1}; & 0 < \sigma_t < \exp(\bar{H}_t) \\ \frac{1}{2\Delta} \exp\left(\frac{\bar{H}_t}{\Delta}\right) \sigma_t^{-1/\Delta-1}; & \sigma_t \geq \exp(\bar{H}_t) \end{cases} \quad (2.1)$$

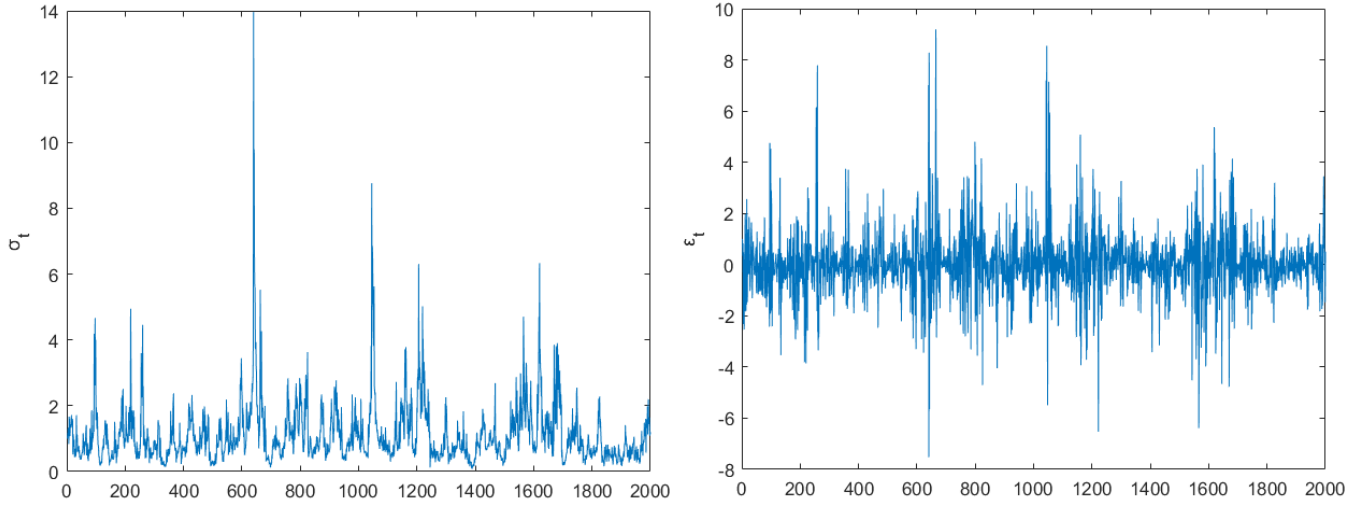


Figure 1: A typical realization of the stochastic volatility σ_t defined in (1.2)-(1.4) and (1.1)'s corresponding process ε_t with $z_t \sim \mathcal{N}(0, 1)$, $H_t = .5H_{t-1} + .4H_{t-2} + h_t$, and $\Delta = 1/4$.

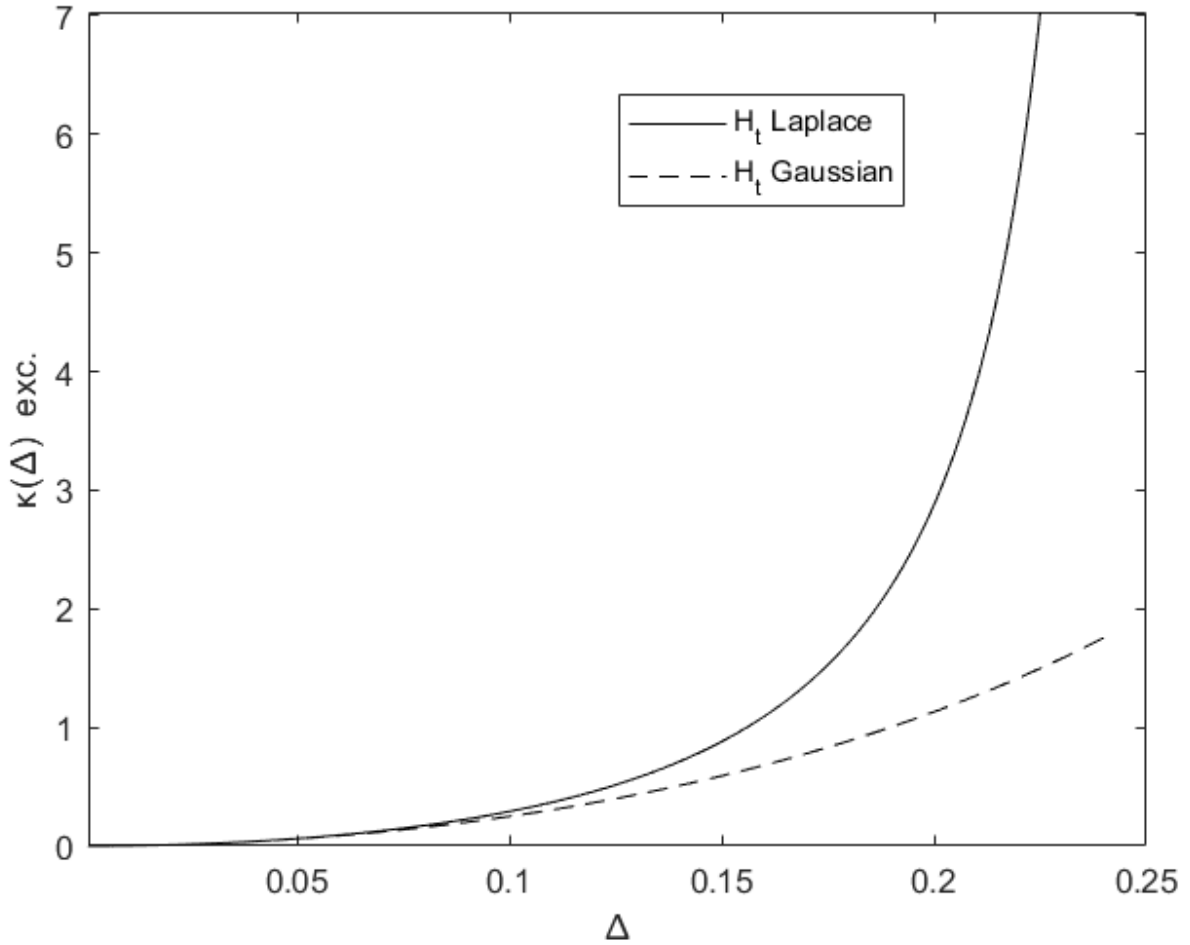


Figure 2: A graph of (2.3)'s conditional excess kurtosis $\kappa^{\text{exc.}}(\Delta) = \kappa(\Delta) - 3$ for Laplace H_t (Solid) along with the corresponding result for Gaussian H_t (Dashed).

Corollary 2.1. *Given (1.1) and (2.1) with $z_t \sim \mathcal{N}(0, 1)$, for all even $n \geq 2$, for $\Delta \geq 1/n$, $E\{\varepsilon_t^n | \mathcal{F}_{t-1}\} = \infty$, while for $\Delta < 1/n$,*

$$E\{\varepsilon_t^n | \mathcal{F}_{t-1}\} = \exp(n\bar{H}_t) \frac{(n-1)!!}{1 - n^2\Delta^2}. \quad (2.2)$$

Several graphs of (2.1) are given in Fig. 3. We note from Corollary 2.1 that the conditional kurtosis $\kappa_t = E\{\varepsilon_t^4 | \mathcal{F}_{t-1}\} / (E\{\varepsilon_t^2 | \mathcal{F}_{t-1}\})^2$ diverges or is not well-defined for $\Delta \geq 1/4$. However, when (2.2) is used to calculate κ_t for $\Delta < 1/4$, it can be easily shown that the conditional kurtosis has the time-independent definition

$$\kappa(\Delta) = 3 \frac{(1 - 4\Delta^2)^2}{1 - 16\Delta^2}, \quad (2.3)$$

which is minimized at $\kappa(0) = 3$, the Gaussian kurtosis. The divergent algebraic structure of (2.3) contrasts with the kurtosis' exponential structure for Gaussian H_t , which would be given by $\kappa_t = 3 \exp(8\Delta^2)$. The *excess kurtosis* $\kappa^{\text{exc.}}(\Delta) = \kappa(\Delta) - 3$ is graphed in Fig. 2 for both Laplace and Gaussian H_t . Now that we have given ε_t 's conditional moment structure, we will present its conditional probability density function and characterize its near-mean and tail behavior.

Theorem 2.1. *Given (2.1) with $z_t \sim \mathcal{N}(0, 1)$, (1.1)'s ε_t is distributed according to the conditional probability density function*

$$p_\varepsilon(\varepsilon_t | \mathcal{F}_{t-1}) = \frac{1}{4\sqrt{\pi}\Delta} \left(\sqrt{2}e^{\bar{H}_t}\right)^{-1/\Delta} \Gamma\left(\frac{1-1/\Delta}{2}, \frac{\varepsilon_t^2}{2e^{2\bar{H}_t}}\right) |\varepsilon_t|^{1/\Delta-1} \\ + \frac{1}{4\sqrt{\pi}\Delta} \left(\sqrt{2}e^{\bar{H}_t}\right)^{1/\Delta} \gamma\left(\frac{1+1/\Delta}{2}, \frac{\varepsilon_t^2}{2e^{2\bar{H}_t}}\right) |\varepsilon_t|^{-1/\Delta-1} \quad (2.4)$$

where

$$\Gamma(a, b) = \int_b^\infty x^{a-1} e^{-x} dx \quad (2.5)$$

is the upper incomplete gamma function and

$$\gamma(a, b) = \int_0^b x^{a-1} e^{-x} dx \quad (2.6)$$

is the lower incomplete gamma function.

Several graphs of (2.4) are given in Fig. 3. Note that with larger Δ and smaller \bar{H}_t the densities are more sharply peaked around the origin. This can also be seen from the following result.

Corollary 2.2. *For $\Delta < 1$, as $|\varepsilon_t| \rightarrow 0$,*

$$p_\varepsilon(\varepsilon_t | \mathcal{F}_{t-1}) \sim \frac{1}{\sqrt{2\pi}e^{\bar{H}_t}} \frac{1}{1 - \Delta^2}. \quad (2.7)$$

It can be seen in the proof of Theorem 2.1 that the piece-wise structure of (2.1) gives (2.4) a structure involving two power law terms. We will next show that the second of these terms is the primary driver of ε_t 's tail behavior.

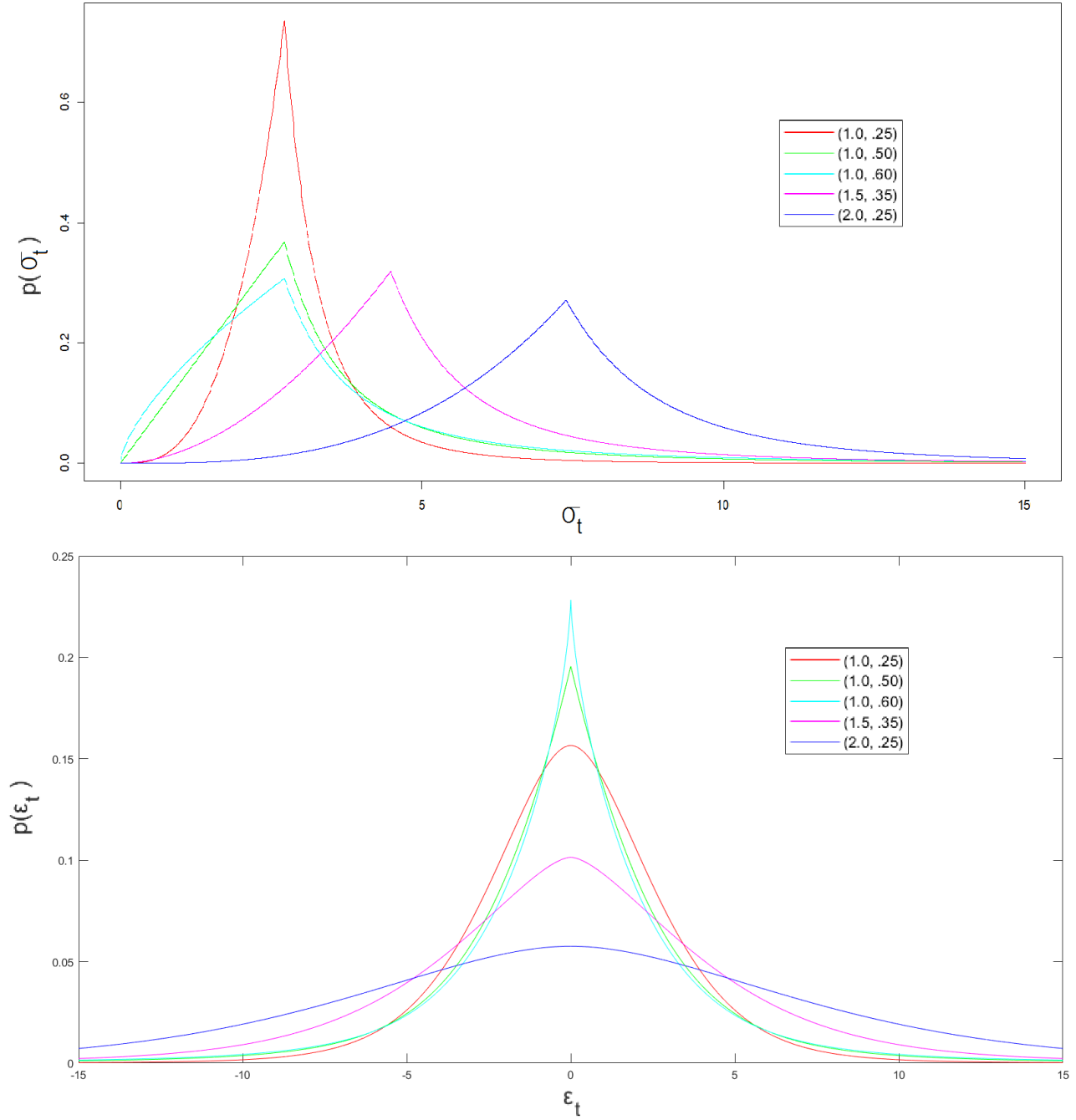


Figure 3: Graphs of the probability density functions (2.1) (Top) and (2.4) (Bottom) with (\bar{H}_t, Δ) equal to (1, .25) in Red, (1, .50) in Green, (1, .60) in Cyan, (1.5, .35) in Magenta, and (2, .25) in Blue.

Theorem 2.2. By (2.4) and (2.1),

$$P\{|\varepsilon_t| \geq \Lambda | \mathcal{F}_{t-1}\} = \frac{1}{2\sqrt{\pi}} \Gamma\left(\frac{1+1/\Delta}{2}\right) \tilde{\Lambda}_t^{-1/\Delta} + O\left(\tilde{\Lambda}_t^{-5} e^{-\tilde{\Lambda}_t^2}\right) \quad (2.8)$$

as

$$\tilde{\Lambda}_t = \frac{\Lambda}{\sqrt{2}e^{\bar{H}_t}} \rightarrow \infty. \quad (2.9)$$

This result reduces to the asymptotic power law in (1.5). We will make extensive use of Theorem 2.2 in our estimation procedure described in the next section. The result arises from asymptotic expansions of (2.4) and its integral $P\{|\varepsilon_t| \geq \Lambda | \mathcal{F}_{t-1}\}$, which are given in (A.15)-(A.17) and (A.22) respectively. We note from integrating (2.1) with $\Lambda \geq \exp(\bar{H}_t)$ that

$$P\{\sigma_t \geq \Lambda | \mathcal{F}_{t-1}\} = \frac{1}{2} \exp\left(\frac{\bar{H}_t}{\Delta}\right) \Lambda^{-1/\Delta}. \quad (2.10)$$

Comparison of (2.10) with (2.8)-(2.9) gives the result

$$P\{|\varepsilon_t| \geq \Lambda | \mathcal{F}_{t-1}\} \sim \frac{\sqrt{2}^{1/\Delta}}{\sqrt{\pi}} \Gamma\left(\frac{1+1/\Delta}{2}\right) P\{\sigma_t \geq \Lambda | \mathcal{F}_{t-1}\}. \quad (2.11)$$

This result shows that, asymptotically, ε_t 's large deviation probabilities are simply proportional to σ_t 's corresponding probabilities through a Δ -dependent factor, and hence the probabilities' dependence on \bar{H}_t is given straightforwardly by $\exp(\bar{H}_t/\Delta)$. It can be seen in (2.8) and (A.22) that more complex dependence on Δ and \bar{H}_t is captured by higher-order terms with comparatively small contributions at high Λ relative to $e^{\bar{H}_t}$. We make the additional note that $\Gamma(3/2) = \sqrt{\pi}/2$ and $\Gamma(1/2) = \sqrt{\pi}$, therefore (2.11) reduces to simply

$$P\{|\varepsilon_t| \geq \Lambda | \mathcal{F}_{t-1}\} \sim P\{\sigma_t \geq \Lambda | \mathcal{F}_{t-1}\}$$

for $\Delta = 1/2$ and as $\Delta \rightarrow \infty$. Now that we have presented the model's polynomial moments and probabilistic structure, we will describe an estimation procedure using some of the above results.

3 Estimation

We begin by considering the conditional expectation of the unobservable quantity H_t , given the value of the observable $\log|\varepsilon_t|$.

Proposition 3.1. Given (1.1) and (1.2),

$$E\{H_t | \log|\varepsilon_t|\} = \log|\varepsilon_t| + \frac{\log 2 + \gamma}{2} \approx \log|\varepsilon_t| + .6352, \quad (3.1)$$

where

$$\gamma = \lim_{n \rightarrow \infty} \left(\sum_{k=1}^n \frac{1}{k} - \log n \right) \approx .5772$$

is the Euler-Mascheroni constant.

By Proposition 3.1, an unbiased estimator for H_t is given by

$$\hat{H}_t = \log |\varepsilon_t| + \frac{\log 2 + \gamma}{2} \approx \log |\varepsilon_t| + .6352. \quad (3.2)$$

An arbitrary regression model $m(\cdot)$ for estimation of $E\{H_t|\mathcal{F}_{t-1}\}$ may then be trained using the \hat{H}_t 's and any other relevant variables $\vec{X}_{t-1}, \dots, \vec{X}_{t-q}$, giving

$$\hat{H}_t = \hat{E}\{H_t|\mathcal{F}_{t-1}\} = m\left(\hat{H}_{t-1}, \dots, \hat{H}_{t-p}, \vec{X}_{t-1}, \dots, \vec{X}_{t-q}, \dots\right). \quad (3.3)$$

We then estimate Δ by finding an approximate solution to the empirical, probabilistic moment constraint

$$\frac{1}{T} \sum_{t=1}^T \mathbb{1}(|\varepsilon_t| \geq \Lambda) = \frac{1}{T} \sum_{t=1}^T \int_{\Lambda}^{\infty} 2p_{\varepsilon}\left(\varepsilon|\hat{H}_t, \hat{\Delta}\right) d\varepsilon, \quad (3.4)$$

where $p_{\varepsilon}(\cdot)$ is given in (2.4) and $\Lambda \in \mathbb{R}^+$. The constraint (3.4) is justified by the law of total expectation, which requires that $E\{\mathbb{1}(|\varepsilon_t| \geq \Lambda)\} = E\{E\{\mathbb{1}(|\varepsilon_t| \geq \Lambda)|\mathcal{F}_{t-1}\}\}$. This Δ -estimation method requires a result for the integral on the right-hand side of (3.4). We will approximate (3.4)'s integral using the asymptotic result in Theorem 2.2, which gives an accurate approximation for sufficiently large $\Lambda/\sqrt{2}e^{\hat{H}_t}$. We therefore use the estimator

$$\hat{\Delta}(\Lambda) = \operatorname{argmin}_{\Delta} \left\{ \left| \sum_{t=1}^T \left(\mathbb{1}(|\varepsilon_t| \geq \Lambda) - \frac{\sqrt{2}^{1/\Delta}}{2\sqrt{\pi}} \Gamma\left(\frac{1+1/\Delta}{2}\right) \exp\left(\frac{\hat{H}_t}{\Delta}\right) \Lambda^{-1/\Delta} \right) \right| \right\} \quad (3.5)$$

In the simulation and empirical sections below, we search for (3.5)'s $\hat{\Delta}$ over the range $[.01, 1]$ with a precision of .01.

4 Simulation

In this section we present results of the estimation procedure described in the previous section for simulations of the process (1.1)-(1.4). We run 1000 simulations each, with sample sizes of 625 and 1250, for Δ ranging from .05 to .50. The model used for (3.3)'s \hat{H}_t is a linear autoregressive model that uses the 10 previous values of (3.2)'s \hat{H}_t . This AR(10) model is calibrated using the Yule-Walker method.

We present simulation results for two different, simple processes for H_t . The first is given by the AR(2) process

$$H_t = .5H_{t-1} + .4H_{t-2} + h_t \quad (4.1)$$

and the second is given by the AR(5) process

$$H_t = .05H_{t-1} + .05H_{t-2} + .25H_{t-3} + .2H_{t-4} + .35H_{t-5} + h_t. \quad (4.2)$$

The results are presented in Table 1, where we give the averages and standard deviations of $\hat{\Delta}$ over the 1000 simulations. For Λ , we choose $2\hat{\sigma}_{\varepsilon}$, $3\hat{\sigma}_{\varepsilon}$, and $4\hat{\sigma}_{\varepsilon}$, where $\hat{\sigma}_{\varepsilon}^2$ is ε_t 's sample variance. This gives a set of data-driven Λ values for which (2.8) is an increasingly accurate approximation of (3.4)'s integral.

One can see in Table 1 that for H_t given by (4.1) (resp. (4.2)) that for $\Delta \leq .30$ (resp. .25), $\hat{\Delta}(k\hat{\sigma}_{\varepsilon})$'s bias appears to decrease as k increases, while for $\Delta > .30$ (resp. .25) the bias seems

Table 1: Estimation results using (3.5)'s $\hat{\Delta}(\Lambda)$, averaged over 1000 simulations of T samples of (1.1)-(1.4) with H_t given by (4.1) and (4.2). Model for (3.3)'s \hat{H}_t is AR(10).

$H_t = (4.1)$											
$T = 625 - 10$											
Δ	.05	.10	.15	.20	.25	.30	.35	.40	.45	.50	
avg. $\hat{\Delta}(2\hat{\sigma}_\varepsilon)$.28	.27	.28	.31	.35	.39	.43	.47	.50	.55	
avg. $\hat{\Delta}(3\hat{\sigma}_\varepsilon)$.14	.16	.20	.26	.32	.37	.41	.47	.51	.56	
avg. $\hat{\Delta}(4\hat{\sigma}_\varepsilon)$.10	.13	.19	.26	.31	.36	.42	.47	.51	.56	
std. dev. $\hat{\Delta}(2\hat{\sigma}_\varepsilon)$.02	.03	.04	.05	.06	.07	.08	.09	.11	.13	
std. dev. $\hat{\Delta}(3\hat{\sigma}_\varepsilon)$.02	.03	.06	.07	.09	.10	.11	.13	.14	.15	
std. dev. $\hat{\Delta}(4\hat{\sigma}_\varepsilon)$.03	.05	.07	.08	.09	.11	.12	.13	.14	.16	
$T = 1250 - 10$											
Δ	.05	.10	.15	.20	.25	.30	.35	.40	.45	.50	
avg. $\hat{\Delta}(2\hat{\sigma}_\varepsilon)$.26	.25	.27	.30	.34	.38	.41	.45	.50	.54	
avg. $\hat{\Delta}(3\hat{\sigma}_\varepsilon)$.13	.15	.21	.27	.32	.37	.41	.46	.51	.55	
avg. $\hat{\Delta}(4\hat{\sigma}_\varepsilon)$.09	.14	.21	.26	.32	.38	.42	.47	.52	.56	
std. dev. $\hat{\Delta}(2\hat{\sigma}_\varepsilon)$.01	.02	.02	.03	.04	.05	.06	.08	.09	.11	
std. dev. $\hat{\Delta}(3\hat{\sigma}_\varepsilon)$.01	.03	.06	.07	.08	.09	.10	.11	.12	.14	
std. dev. $\hat{\Delta}(4\hat{\sigma}_\varepsilon)$.02	.05	.06	.07	.08	.09	.10	.12	.14	.14	
$H_t = (4.2)$											
$T = 625 - 10$											
Δ	.05	.10	.15	.20	.25	.30	.35	.40	.45	.50	
avg. $\hat{\Delta}(2\hat{\sigma}_\varepsilon)$.29	.27	.26	.26	.28	.32	.36	.41	.46	.52	
avg. $\hat{\Delta}(3\hat{\sigma}_\varepsilon)$.15	.14	.17	.21	.26	.32	.38	.43	.48	.52	
avg. $\hat{\Delta}(4\hat{\sigma}_\varepsilon)$.10	.11	.15	.20	.26	.32	.37	.42	.48	.53	
std. dev. $\hat{\Delta}(2\hat{\sigma}_\varepsilon)$.02	.02	.03	.03	.05	.07	.09	.10	.12	.12	
std. dev. $\hat{\Delta}(3\hat{\sigma}_\varepsilon)$.02	.02	.04	.06	.08	.08	.09	.10	.10	.12	
std. dev. $\hat{\Delta}(4\hat{\sigma}_\varepsilon)$.02	.04	.06	.07	.08	.08	.08	.09	.10	.11	
$T = 1250 - 10$											
Δ	.05	.10	.15	.20	.25	.30	.35	.40	.45	.50	
avg. $\hat{\Delta}(2\hat{\sigma}_\varepsilon)$.27	.26	.25	.25	.27	.32	.36	.41	.46	.52	
avg. $\hat{\Delta}(3\hat{\sigma}_\varepsilon)$.13	.13	.17	.23	.28	.33	.38	.43	.48	.53	
avg. $\hat{\Delta}(4\hat{\sigma}_\varepsilon)$.09	.11	.16	.22	.28	.33	.38	.43	.48	.53	
std. dev. $\hat{\Delta}(2\hat{\sigma}_\varepsilon)$.01	.02	.02	.03	.05	.06	.08	.09	.10	.11	
std. dev. $\hat{\Delta}(3\hat{\sigma}_\varepsilon)$.01	.02	.05	.06	.07	.07	.08	.08	.09	.10	
std. dev. $\hat{\Delta}(4\hat{\sigma}_\varepsilon)$.02	.04	.05	.06	.06	.07	.07	.08	.08	.10	

to remain constant or slightly increase with k . The estimator's variance appears to nearly always increase with k , which is likely due to the higher variance in probability estimates for larger deviations. It is also clear that the variance increases with Δ , which could be related to the increased variance in $\hat{\sigma}_\varepsilon$ for larger Δ . Doubling the sample size decreased the estimators' standard deviations by .01 to .02, and had a similar effect on the some of the biases. Although the bias actually increased in many cases by increasing the sample size.

The estimator $\hat{\Delta}(2\hat{\sigma}_\varepsilon)$'s bias is very large for small Δ and decreases greatly as $\Delta \rightarrow 1/2$. This is possibly because as Δ increases, (2.4) becomes sharper around the origin, and hence $2\hat{\sigma}_\varepsilon$ is sufficiently far in the tails for (2.8) to be a good approximation to (3.4)'s integral. Meanwhile for $k = 3$ and 4, $\hat{\Delta}(k\hat{\sigma}_\varepsilon)$'s bias appears to be minimal around $.10 \leq \Delta \leq .2$. The inherent upward bias in the $\hat{\Delta}$'s is likely due to model error in \hat{H}_t , since decreased predictability of H_t manifests as a higher empirical Δ . This explains the increases in bias seen when doubling the sample size, because the AR(10) models for \hat{H}_t overfitted the data less on the larger samples.

The processes (4.1)-(4.2) were selected for their simplicity and the superficial similarity between their short-term autocorrelation structure and those seen in financial data sets. In particular, (4.1) and (4.2)'s corresponding $|\varepsilon_t|$'s appear to be slightly more strongly locally correlated, but otherwise their short-term autocorrelations resemble those seen in recent daily S&P 500 and U.S. Dollar/Euro absolute log-returns. Hence these simulation results show that with a realistically sized sample and similar conditions to the application below, $\hat{\Delta}(k\hat{\sigma}_\varepsilon)$ with $k = 3$ or 4 can provide a computationally inexpensive and satisfactory estimate of Δ , given a predictive model for H_t .

5 Empirical Application

In this section we apply our modeling and estimation procedure to daily log-returns of the S&P 500 Index (SPX). We consider approximately 5 years of data from February 27, 2014 to February 14, 2019, giving 1,250 total samples. We build a sparse, linear regression model for (3.3)'s \hat{H}_t using two sets of covariates. The first set is the 10 previous values of (3.2)'s \hat{H}_t , $\{\hat{H}_{t-1}, \dots, \hat{H}_{t-10}\}$. The second set is the 10 previous values of $\log(\text{VIX}_t)$, $\{\log(\text{VIX}_{t-1}), \dots, \log(\text{VIX}_{t-10})\}$, where VIX refers to the Chicago Board Options Exchange (CBOE) Volatility Index, which is an implied volatility measure computed from SPX option prices. It is perhaps the most well-known and widely disseminated measure of implied volatility for the S&P 500 Index.

Because of high correlation and potential multicollinearity in the model's set of explanatory variables

$$\left\{ \hat{H}_{t-1}, \dots, \hat{H}_{t-10}, \log(\text{VIX}_{t-1}), \dots, \log(\text{VIX}_{t-10}) \right\}, \quad (5.1)$$

we proceed by applying Principal Component Analysis (PCA) to this data to create the uncorrelated Principal Components (PCs) $\phi_t^{(1)}, \dots, \phi_t^{(20)}$. We then use Tibshirani's (1996) LASSO regression and Friedman et. al.'s (2010) cyclic coordinate descent to give the model

$$\hat{H}_t = \hat{\beta}_0 + \sum_{n=1}^{20} \hat{\beta}_n \phi_t^{(n)}, \quad (5.2)$$

where

$$\hat{\beta} = \underset{\beta}{\operatorname{argmin}} \left\{ \frac{1}{2T} \sum_{t=11}^{T+10} \left| \hat{H}_t - \beta_0 - \sum_{n=1}^{20} \beta_n \phi_t^{(n)} \right|^2 + \lambda \sum_{n=1}^{20} |\beta_n| \right\}, \quad (5.3)$$

and λ minimizes \widehat{H}_t 's mean absolute 10-fold cross-validation error. This procedure, which can be called L1-penalized PC Regression, gives a sparse linear model for \widehat{H}_t . We will use this simple model with (3.5)'s $\widehat{\Delta} = \widehat{\Delta}(4\widehat{\sigma}_\varepsilon)$ to give an estimate of ε_t 's next-day volatility $\widehat{\sigma}_{\varepsilon,t} = \sqrt{E\{\varepsilon_t^2|\mathcal{F}_{t-1}\}}$ as well as a dynamic estimate of the probability that $|\varepsilon_t| \geq 3\widehat{\sigma}_\varepsilon$.

We use the moment result (2.2) to give the following model for the next-day volatility:

$$\widehat{\sigma}_{\varepsilon,t} = \sqrt{E\{\varepsilon_t^2|\widehat{H}_t, \widehat{\Delta}\}} = \exp\left(\widehat{H}_t\right) \sqrt{\frac{1}{1 - 4\widehat{\Delta}^2}}. \quad (5.4)$$

We additionally use the asymptotic result (2.8)-(2.9) to give the dynamic probability estimate

$$\widehat{P}\left\{|\varepsilon_t| \geq 3\widehat{\sigma}_\varepsilon|\widehat{H}_t, \widehat{\Delta}\right\} = \frac{\sqrt{2^{1/\widehat{\Delta}}}}{2\sqrt{\pi}} \Gamma\left(\frac{1 + 1/\widehat{\Delta}}{2}\right) \exp\left(\frac{\widehat{H}_t}{\widehat{\Delta}}\right) (3\widehat{\sigma}_\varepsilon)^{-1/\widehat{\Delta}}. \quad (5.5)$$

To measure the predictive capability of (5.4) we use the empirical correlation

$$\rho_{|\varepsilon|, \widehat{\sigma}} = \text{corr}\left\{|\varepsilon_t|, \widehat{\sigma}_{\varepsilon,t}\right\}. \quad (5.6)$$

To measure the predictiveness of (5.5), we use it to create a classifier. We begin by noting that the stationary probability that $|\varepsilon_t| \geq 3\widehat{\sigma}_\varepsilon$ under a Gaussian distribution is $\approx .0027$. We then use (5.5) to define a binary classifier ξ_t with the form

$$\xi_t = \begin{cases} 1; & \widehat{P}\left\{|\varepsilon_t| \geq 3\widehat{\sigma}_\varepsilon|\widehat{H}_t, \widehat{\Delta}\right\} \geq 5 \times .0027 \\ 0; & \widehat{P}\left\{|\varepsilon_t| \geq 3\widehat{\sigma}_\varepsilon|\widehat{H}_t, \widehat{\Delta}\right\} < 5 \times .0027 \end{cases} \quad (5.7)$$

Hence ξ_t identifies days when the probability that $|\varepsilon_t| \geq 3\widehat{\sigma}_\varepsilon$ exceeds 5 times the stationary Gaussian probability. We then calculate ξ_t 's sensitivity (Sn.) and specificity (Sp.), which are defined here as

$$\text{Sn.} = \frac{|\{\varepsilon_t \text{ s.t. } |\varepsilon_t| \geq 3\widehat{\sigma}_\varepsilon \wedge \xi_t = 1\}|}{|\{\varepsilon_t \text{ s.t. } |\varepsilon_t| \geq 3\widehat{\sigma}_\varepsilon\}|} \quad (5.8)$$

and

$$\text{Sp.} = \frac{|\{\varepsilon_t \text{ s.t. } |\varepsilon_t| < 3\widehat{\sigma}_\varepsilon \wedge \xi_t = 0\}|}{|\{\varepsilon_t \text{ s.t. } |\varepsilon_t| < 3\widehat{\sigma}_\varepsilon\}|}. \quad (5.9)$$

The measure (5.8) gives the percentage of 3 standard deviation days correctly predicted by ξ_t , while (5.9) gives the percentage of non-3 standard deviation days correctly predicted by ξ_t .

We evaluate our modeling using backtesting. In particular we do two sets of backtests. In the first backtesting exercise, we train the model on the first 50% of the data, or 625 samples from February 27, 2014 to August 18, 2016. We then test the model's performance on the second 50% or 625 samples of the data. In the second backtesting exercise we train the model on the first 60% of the data, or 750 samples from February 27, 2014 to February 17, 2017. We test the model's performance on the second 40% or 500 samples of the data. We run both backtests 100 times each and list averages of (3.5)'s $\widehat{\Delta}(4\widehat{\sigma}_\varepsilon)$, (5.6)'s $\rho_{|\varepsilon|, \widehat{\sigma}}$, and (5.8)-(5.9) in Table 2.

It is clear from Table 2 that the modeling is highly predictive of extreme events in daily fluctuations of the S&P 500 Index. In particular, (5.5) and (5.7)'s naive classifier ξ_t on average correctly predicts 85% of 3 standard deviation events out-of-sample, and was observed to predict as high as 91% of such events. The classifier does this while still maintaining a high specificity of 76% on average, with

Table 2: SPX Backtesting Results: Averages (\pm Standard Deviation)

$N_{\text{Train}}/N_{\text{Test}}$	avg. $\widehat{\Delta}(4\widehat{\sigma}_\varepsilon)$	avg. $\rho_{ \varepsilon ,\widehat{\sigma}}$	avg. Sn.	avg. Sp.
625/625 (50/50)	.33 (\pm .03)	.39 (\pm .02)	.78 (\pm .00)	.74 (\pm .04)
750/500 (60/40)	.28 (\pm .02)	.47 (\pm .01)	.85 (\pm .05)	.76 (\pm .02)

an observed range of 71% to 80%. We also note that (5.4)’s $\widehat{\sigma}_{\varepsilon,t}$ achieves nearly 50% correlation with $|\varepsilon_t|$ out-of-sample, which shows the modeling’s ability to predict fluctuations in volatility.

We make the note that, by Theorem 2.2, the approximation (5.5) diverges beyond unity for high values of \widehat{H}_t . In particular, on the 50/50 test set, (5.5) exceeds unity 5 times on average, while on the 60/40 test set it does so 3 times on average. In such extreme environments (5.5) cannot be relied upon to give accurate probability estimates. Rather, (2.8)-(2.9) and corresponding estimates with the form of (5.5) can be used as early warning tools for upcoming extreme events.

We additionally note that since the model (5.2)-(5.3) uses the 10 previous values of \widehat{H}_t and $\log(\text{VIX}_t)$, it has a memory length of about two trading weeks. This relatively naive, short-memory modeling of H_t could potentially be improved for this application, since many researchers have found empirical evidence of long-memory in SPX volatility (see Ding et. al. 1993, Bollerslev and Mikkelsen 1996, Lobato and Savin 1998, Ray and Tsay 2000, Grau-Carles 2000). The modeling could also be adjusted to accomodate the asymmetric tails observed in stock market data, often called the “leverage effect” (see Black 1976, Christie 1982, Nelson 1991, Engle and Ng 1993). Overall, though, the study here shows that a simple, short-memory model for H_t that uses only recent realized and implied volatility measures, with the parametrization (1.1)-(1.5), can enable straightforward and predictive tail inference in financial time series. Plots of the SPX log-returns along with corresponding volatility and probability estimates are given in Fig.4.

6 Conclusion

We have presented a family of stochastic volatility models that enable dynamic tail inference in heavy-tailed time series. The family’s conditional probabilistic structure allows for straightforward, effective, and computationally inexpensive estimation of model parameters and outcome probabilities. We have shown that this modeling formalism can be useful for predictive inference of dynamically changing extreme event probabilities in financial time series data. Current and future directions of research involve long-memory modeling for conditionally Laplace processes, accomodation of asymmetric volatility and tails, and generalization of this formalism to the multivariate case.

Acknowledgements

The author thanks Prof. Gennady Samorodnitsky, Cornell University, and Prof. Richard Davis, Columbia University, for their comments on a very early version of this work in 2016. The author is also very grateful to Dr. Dobrislav Dobrev, Federal Reserve Board, for very helpful comments on an early version of this manuscript at the 2017 10th Annual Society for Financial Econometrics (SoFiE) Conference. The author also thanks Prof. Richard Kleeman, Courant Institute of Mathematical Sciences, and Prof. Clifford Hurvich, NYU Stern, for many hours of motivating discussions, along with Prof. Fahad Saled, McGill University, and Franz Hinzen, NYU Stern, for encouragement and conversation on these topics. Finally, the author is very grateful to Prof. David Jablons, University of California San Francisco, for his generous encouragement and support.

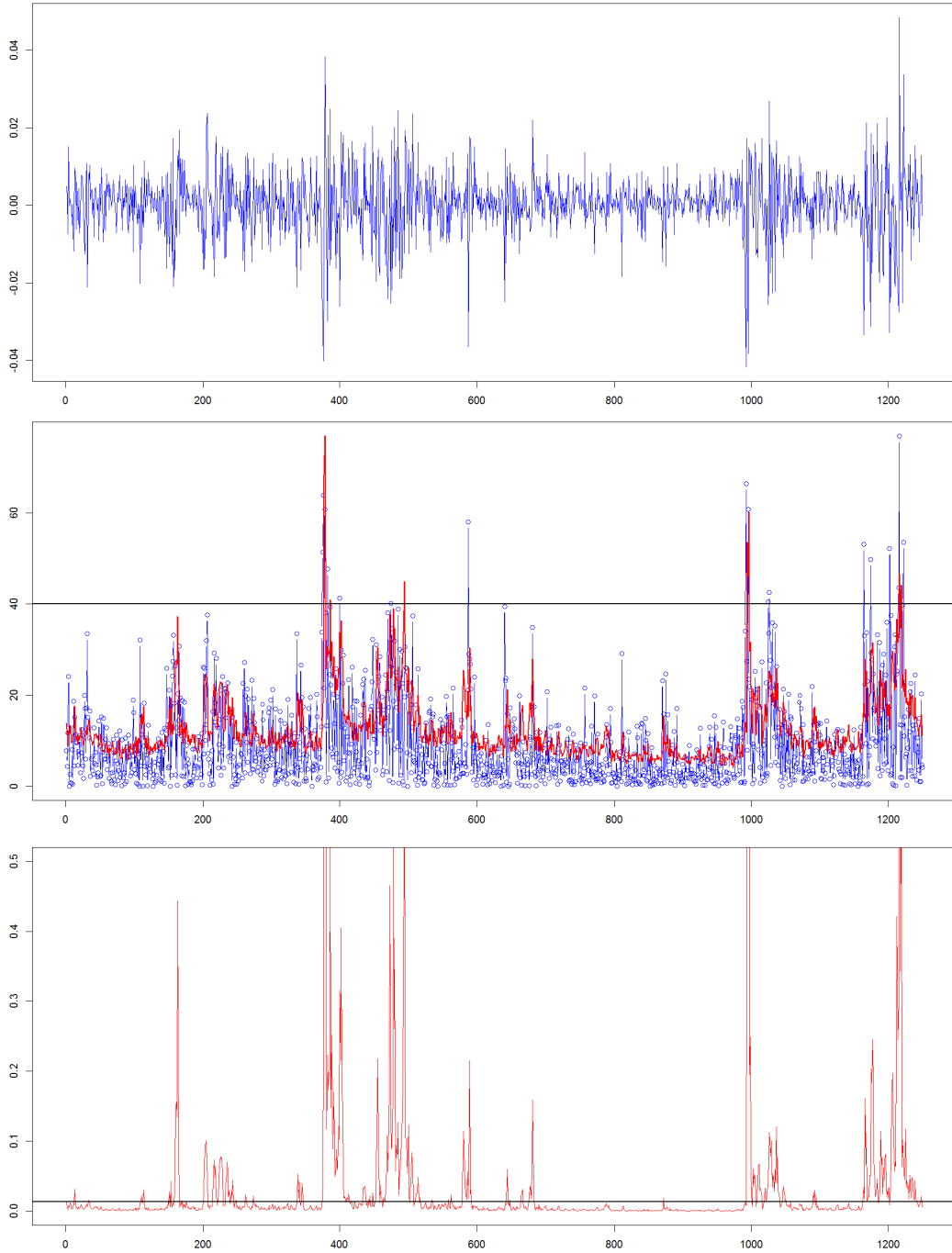


Figure 4: Top Row: SPX log-returns ε_t . Middle Row: Annualized $|\varepsilon_t|$ in Blue and (5.4)'s $\hat{\sigma}_{\varepsilon,t}$ in Red with $3\hat{\sigma}_\varepsilon$ marked in Black. Bottom Row: (5.5)'s $\hat{P}\left\{|\varepsilon_t| \geq 3\hat{\sigma}_\varepsilon | \hat{H}_t, \hat{\Delta}\right\}$ in Red with the threshold value for (5.7)'s ξ_t marked in Black. \hat{H}_t is the model defined in (5.2)-(5.3), while $\hat{\Delta}$ is (3.5)'s $\hat{\Delta}(4\hat{\sigma}_\varepsilon)$. The whole-sample result is $\hat{\Delta}_{\text{SPX}} = .28$.

A Appendix 1: Proofs

A.1 Proof of Lemma 2.1

Proof. We first make the substitution $y = \log(y'/e^{\bar{H}_t})$. Then by (1.2) and (1.4), for $h_t \geq 0$,

$$P(\sigma_t \leq y') = P(h_t \leq y) = \frac{1}{2} - \frac{1}{2} \exp\left(-\frac{\log(e^{-\bar{H}_t} y')}{\Delta}\right) = \frac{1}{2} - \frac{1}{2} \left(\frac{e^{\bar{H}_t}}{y'}\right)^{\frac{1}{\Delta}}$$

We then differentiate w.r.t. y' and let $y' = \sigma_t$, which gives (2.1)'s result for $\sigma_t \geq \exp(\bar{H}_t)$. Next, by (1.2), (1.4), for $h_t < 0$,

$$P(\sigma_t \leq y') = P(h_t \leq y) = \frac{1}{2} \exp\left(\frac{\log(e^{-\bar{H}_t} y')}{\Delta}\right) = \frac{1}{2} \left(\frac{y'}{e^{\bar{H}_t}}\right)^{\frac{1}{\Delta}}.$$

We again differentiate w.r.t. y' and let $y' = \sigma_t$ to give (2.1)'s result for $0 \leq \sigma_t < \exp(\bar{H}_t)$. \square

A.2 Proof of Corollary 2.1

Proof. We note from (2.1) that for any $n \geq 1$, the conditional expected value of σ_t^n is equal to the sum of integrals

$$E\{\sigma_t^n | \mathcal{F}_{t-1}\} = \frac{1}{2\Delta} \left(\exp\left(-\frac{\bar{H}_t}{\Delta}\right) \int_0^{\exp(\bar{H}_t)} \sigma_t^{1/\Delta+n-1} d\sigma_t + \exp\left(\frac{\bar{H}_t}{\Delta}\right) \int_{\exp(\bar{H}_t)}^\infty \sigma_t^{-1/\Delta+n-1} d\sigma_t \right),$$

the second term of which diverges for $\Delta \geq 1/n$, while for $\Delta < 1/n$ we have after integration

$$E\{\sigma_t^n | \mathcal{F}_{t-1}\} = \frac{1}{2} \exp(n\bar{H}_t) \left(\frac{1}{1-n\Delta} + \frac{1}{1+n\Delta} \right) = \frac{\exp(n\bar{H}_t)}{1-n^2\Delta^2}, \quad (\text{A.1})$$

We next note that since z_t is *i.i.d.* and z_t and σ_t are independent, the conditional expectation $E\{\varepsilon_t^n | \mathcal{F}_{t-1}\} = E z_t^n E\{\sigma_t^n | \mathcal{F}_{t-1}\}$. Since z_t is standard normal, its n th moment is simply $(n-1)!! = (n-1)(n-3)(n-5)\dots 1$. Therefore $E\{\varepsilon_t^n | \mathcal{F}_{t-1}\} = (n-1)!! E\{\sigma_t^n | \mathcal{F}_{t-1}\}$. Using (A.1) then gives (2.2)'s result. \square

A.3 Proof of Theorem 2.1

Proof. We note from Rohatgi (1976 p. 141) that since (1.1)'s z_t and σ_t are independent, the distribution of their product $\sigma_t z_t = \varepsilon_t$ is given by the formula

$$p_\varepsilon(\varepsilon_t | \mathcal{F}_{t-1}) = \int_0^\infty p_\sigma(\sigma_t | \mathcal{F}_{t-1}) p_z\left(\frac{\varepsilon_t}{\sigma_t}\right) \frac{1}{|\sigma_t|} d\sigma_t. \quad (\text{A.2})$$

We then substitute the standard normal density for p_z and (2.1) for p_σ into (A.2) to give

$$\begin{aligned} p_\varepsilon(\varepsilon_t | \mathcal{F}_{t-1}) &= \frac{1}{2\Delta\sqrt{2\pi}} \exp\left(-\frac{\bar{H}_t}{\Delta}\right) \int_0^{\exp(\bar{H}_t)} \sigma_t^{1/\Delta-2} e^{-\frac{\varepsilon_t^2}{2\sigma_t^2}} d\sigma_t \\ &\quad + \frac{1}{2\Delta\sqrt{2\pi}} \exp\left(\frac{\bar{H}_t}{\Delta}\right) \int_{\exp(\bar{H}_t)}^\infty \sigma_t^{-1/\Delta-2} e^{-\frac{\varepsilon_t^2}{2\sigma_t^2}} d\sigma_t \end{aligned} \quad (\text{A.3})$$

We note from (2.5) that the first integral in (A.3) can be written in the following form after simplifying

$$\frac{(\sqrt{2}e^{\bar{H}_t})^{-1/\Delta}}{4\sqrt{\pi}\Delta} |\varepsilon_t|^{1/\Delta-1} \left[\Gamma\left(\frac{1-1/\Delta}{2}, \frac{\varepsilon_t^2}{2\sigma_t^2}\right)_{\sigma_t=e^{\bar{H}_t}} - \Gamma\left(\frac{1-1/\Delta}{2}, \frac{\varepsilon_t^2}{2\sigma_t^2}\right)_{\sigma_t=0} \right] \quad (\text{A.4})$$

To simplify (A.4) further, we note from Abramowitz and Stegun (1965 p. 263) that the upper incomplete gamma function satisfies

$$\Gamma(a, b) \sim b^{a-1}e^{-b} \quad (\text{A.5})$$

as $b \rightarrow \infty$. Letting $(1-1/\Delta)/2 = a$ and $\varepsilon_t^2/2\sigma_t^2 = b$ in (A.5) shows that the second term in (A.4) vanishes. Final simplification of (A.4) gives the result

$$\frac{1}{4\sqrt{\pi}\Delta} (\sqrt{2}e^{\bar{H}_t})^{-1/\Delta} \Gamma\left(\frac{1-1/\Delta}{2}, \frac{\varepsilon_t^2}{2e^{2\bar{H}_t}}\right) |\varepsilon_t|^{1/\Delta-1}. \quad (\text{A.6})$$

The definition (2.5) can be used again to write the second integral in (A.3) as

$$\frac{(\sqrt{2}e^{\bar{H}_t})^{1/\Delta}}{4\sqrt{\pi}\Delta} |\varepsilon_t|^{-1/\Delta-1} \left[\Gamma\left(\frac{1+1/\Delta}{2}, \frac{\varepsilon_t^2}{2\sigma_t^2}\right)_{\sigma_t=\infty} - \Gamma\left(\frac{1+1/\Delta}{2}, \frac{\varepsilon_t^2}{2\sigma_t^2}\right)_{\sigma_t=e^{\bar{H}_t}} \right] \quad (\text{A.7})$$

after simplifying. The first upper incomplete gamma function term in (A.7) is simply $\Gamma((1+1/\Delta)/2)$. We then note that

$$\Gamma(a) - \Gamma(a, b) = \gamma(a, b). \quad (\text{A.8})$$

Using this identity with (A.7) and simplifying gives

$$\frac{1}{4\sqrt{\pi}\Delta} (\sqrt{2}e^{\bar{H}_t})^{1/\Delta} \gamma\left(\frac{1+1/\Delta}{2}, \frac{\varepsilon_t^2}{2e^{2\bar{H}_t}}\right) |\varepsilon_t|^{-1/\Delta-1}. \quad (\text{A.9})$$

Adding (A.6) and (A.9) gives the result in (2.4). \square

A.4 Proof of Corollary 2.2

Proof. We first note the identity shown in Jameson (2016, 2017)

$$\Gamma(a, b) \sim -\frac{b^a}{a} \quad (\text{A.10})$$

as $b \rightarrow 0$ for $a < 0$. For $\Delta < 1$, $(1-1/\Delta)/2 < 0$, and hence using (A.10) and rewriting gives

$$\Gamma\left(\frac{1-1/\Delta}{2}, \frac{\varepsilon_t^2}{2e^{2\bar{H}_t}}\right) \sim \frac{2\Delta}{1-\Delta} \left(\frac{|\varepsilon_t|}{\sqrt{2}e^{\bar{H}_t}}\right)^{1-1/\Delta} \quad (\text{A.11})$$

as $|\varepsilon_t| \rightarrow 0$. We next note the identity

$$\gamma(a, b) \sim \frac{b^a}{a} \quad (\text{A.12})$$

as $b \rightarrow 0$. Using (A.12) and rewriting then gives

$$\gamma\left(\frac{1+1/\Delta}{2}, \frac{\varepsilon_t^2}{2e^{2\bar{H}_t}}\right) \sim \frac{2\Delta}{1+\Delta} \left(\frac{|\varepsilon_t|}{\sqrt{2}e^{\bar{H}_t}}\right)^{1+1/\Delta} \quad (\text{A.13})$$

as $|\varepsilon_t| \rightarrow 0$. Substituting (A.11) and (A.13) into (2.4) and cancelling terms gives

$$p_\varepsilon(\varepsilon_t|\mathcal{F}_{t-1}) \sim \frac{1}{4}\sqrt{\frac{2}{\pi}}\frac{1}{e^{\bar{H}_t}} \left(\frac{1}{1-\Delta} + \frac{1}{1+\Delta}\right)$$

as $|\varepsilon_t| \rightarrow 0$, which can be simplified to give the result (2.7). \square

A.5 Proof of Theorem 2.2

Proof. We begin with the following asymptotic expansion of (2.5), available at the National Institute of Standards and Technology's Digital Library of Mathematical Functions:

$$\Gamma(a, b) = b^{a-1} e^{-b} \left(1 + \sum_{k=1}^{n-1} \frac{u_k(a)}{b^k} + O(b^{-n}) \right) \quad (\text{A.14})$$

as $b \rightarrow \infty$, where

$$u_k(a) = (a-k)(a-k+1)\dots(a-2)(a-1). \quad (\text{A.15})$$

We then make the following substitutions in (2.4),

$$a_1 = \frac{1-1/\Delta}{2}, \quad a_2 = \frac{1+1/\Delta}{2}, \quad b_t = \frac{\varepsilon_t^2}{2e^{2\bar{H}_t}}. \quad (\text{A.16})$$

We then recall (A.8) and substitute (A.14) into (2.4)'s two terms (A.6) and (A.9). Simplifying then gives the series representation of (2.4) as $b_t \rightarrow \infty$,

$$p_\varepsilon(\varepsilon_t | \mathcal{F}_{t-1}) = \frac{1}{4\Delta\sqrt{2\pi}e^{\bar{H}_t}} \left(b_t^{-a_2} \Gamma(a_2) + b_t^{-1} e^{-b_t} \sum_{k=1}^{n-1} \frac{u_k(a_1) - u_k(a_2)}{b_t^k} + O(b_t^{-n-1} e^{-b_t}) \right). \quad (\text{A.17})$$

We next note that, after re-substituting for b_t and a_2 , the first term in (A.17) is equal to

$$\frac{1}{4\sqrt{\pi}\Delta} \left(\sqrt{2}e^{\bar{H}_t} \right)^{1/\Delta} \Gamma\left(\frac{1+1/\Delta}{2}\right) |\varepsilon_t|^{-1/\Delta-1}, \quad (\text{A.18})$$

which is the limit of the term (A.9) as $|\varepsilon_t| \rightarrow \infty$. Multiplying (A.18) by 2 and integrating from Λ to ∞ gives the first term of (2.8) with (2.9). We then proceed to (A.17)'s second term, re-substituting for b_t and cancelling factors to give

$$\frac{e^{\bar{H}_t}}{2\Delta\sqrt{2\pi}} \frac{e^{-\varepsilon_t^2/2e^{2\bar{H}_t}}}{\varepsilon_t^2} \sum_{k=1}^{n-1} \frac{u_k(a_1) - u_k(a_2)}{\varepsilon_t^{2k}} \left(2e^{2\bar{H}_t} \right)^k. \quad (\text{A.19})$$

We next note the following integral,

$$\int_{\Lambda}^{\infty} e^{-\varepsilon^2/2e^{2\bar{H}_t}} \varepsilon^{-2(k+1)} d\varepsilon = \frac{1}{2} \left(2e^{2\bar{H}_t} \right)^{-k-1/2} \Gamma\left(-k - \frac{1}{2}, \frac{\Lambda^2}{2e^{2\bar{H}_t}}\right). \quad (\text{A.20})$$

So integrating (A.19) from Λ to ∞ , applying (A.20), and cancelling factors gives

$$\frac{1}{8\sqrt{\pi}\Delta} \sum_{k=1}^{n-1} [u_k(a_1) - u_k(a_2)] \Gamma\left(-k - \frac{1}{2}, \frac{\Lambda^2}{2e^{2\bar{H}_t}}\right). \quad (\text{A.21})$$

We then similarly apply (A.20) for the integral of (A.17)'s remainder term. Finally, multiplying (A.17) by 2 and integrating from Λ to ∞ , applying the integral of (A.18), the result (A.21), and fully re-substituting gives the asymptotic expansion

$$\begin{aligned} P\{|\varepsilon_t| \geq \Lambda | \mathcal{F}_{t-1}\} &= \frac{\sqrt{2}^{1/\Delta}}{2\sqrt{\pi}} \Gamma\left(\frac{1+1/\Delta}{2}\right) \exp\left(\frac{\bar{H}_t}{\Delta}\right) \Lambda^{-1/\Delta} \\ &+ \frac{1}{4\sqrt{\pi}\Delta} \sum_{k=1}^{n-1} \left[u_k\left(\frac{1-1/\Delta}{2}\right) - u_k\left(\frac{1+1/\Delta}{2}\right) \right] \Gamma\left(-k - \frac{1}{2}, \frac{\Lambda^2}{2e^{2\bar{H}_t}}\right) \\ &+ O\left(\Gamma\left(-n - \frac{1}{2}, \frac{\Lambda^2}{2e^{2\bar{H}_t}}\right)\right). \end{aligned} \quad (\text{A.22})$$

Re-applying (A.14) to (A.22)'s remainder term gives the remainder term in (2.8) with (2.9). \square

A.6 Proof of Proposition 3.1

Proof. By (1.1) and (1.2), $|\varepsilon_t| = \exp(H_t) |z_t|$. Taking the logarithm gives

$$\log |\varepsilon_t| = H_t + \log |z_t|. \quad (\text{A.23})$$

Since z_t and ε_t are independent, $E \{\log |z_t| | \log |\varepsilon_t|\} = E \log |z_t|$. Then since z_t is standard normal, $z_t^2 \sim \chi^2(1)$. It can then be noted, e.g., from Breidt et. al. (1998) that

$$E \log |z_t| = \frac{1}{2} E \log z_t^2 = \frac{1}{2} \left(\log 2 + \psi \left(\frac{1}{2} \right) \right) = \frac{-\log 2 - \gamma}{2} \approx -.6352, \quad (\text{A.24})$$

where $\psi(x)$ is the *digamma function* (see Abramowitz and Stegun 1965 p. 258-259). Rearranging (A.23), taking the expected value $E \{H_t | \log |\varepsilon_t|\}$, and substituting (A.24) gives the result (3.1). \square

B Appendix 2: The $z_t \sim \text{Lap}(0, 1)$ Case

In this section we briefly show that very similar results to those in Appendix 1 for (1.1)-(1.4) with $z_t \sim \mathcal{N}(0, 1)$ can be derived for the case where z_t is instead distributed according to the standard Laplace density

$$p_z(z_t) = \frac{1}{2} \exp(-|z_t|), \quad (\text{B.1})$$

which gives $E z_t = 0$ and $E |z_t| = 1$. We first note that an equivalent argument to that in A.2 can be made. We use the fact that (B.1)'s $E z_t^n = n!$ with the result (A.1) to give

$$E \{\varepsilon_t^n | \mathcal{F}_{t-1}\} = \exp(n \bar{H}_t) \frac{n!}{1 - n^2 \Delta^2} \quad (\text{B.2})$$

for even $n \geq 2$. The right hand side of (B.2) with $n = 1$ additionally gives $E \{|\varepsilon_t| | \mathcal{F}_{t-1}\}$.

We next note that an equivalent argument to the one in A.3 can be given, using (2.1) and (B.1) with (A.2) to give an expression composed of two integrals, each of which can be written very similarly to (A.4) and (A.7). Then (A.5) and (A.8) can be used in the same way as above to simplify these terms. Adding these two terms gives the result

$$\begin{aligned} p_\varepsilon(\varepsilon_t | \mathcal{F}_{t-1}) &= \frac{1}{4\Delta} \exp\left(-\frac{\bar{H}_t}{\Delta}\right) \Gamma\left(1 - \frac{1}{\Delta}, \frac{|\varepsilon_t|}{e^{\bar{H}_t}}\right) |\varepsilon_t|^{1/\Delta-1} \\ &\quad + \frac{1}{4\Delta} \exp\left(\frac{\bar{H}_t}{\Delta}\right) \gamma\left(1 + \frac{1}{\Delta}, \frac{|\varepsilon_t|}{e^{\bar{H}_t}}\right) |\varepsilon_t|^{-1/\Delta-1} \end{aligned} \quad (\text{B.3})$$

The identities (A.10) and (A.12) in A.4 can then be used to show that as $|\varepsilon_t| \rightarrow 0$,

$$p_\varepsilon(\varepsilon_t | \mathcal{F}_{t-1}) \sim \frac{1}{2e^{\bar{H}_t}} \frac{1}{1 - \Delta^2}. \quad (\text{B.4})$$

The argument in A.5 can also be repeated, using (A.14)-(A.15) with the substitutions

$$a_1 = 1 - \frac{1}{\Delta}, \quad a_2 = 1 + \frac{1}{\Delta}, \quad b_t = \frac{|\varepsilon_t|}{e^{\bar{H}_t}}$$

to write $p_\varepsilon(\varepsilon_t | \mathcal{F}_{t-1})$ as an asymptotic expansion that is equivalent in form to (A.17), with the only change being that the factor $1/(4\Delta\sqrt{2\pi}e^{\bar{H}_t})$ is replaced with $1/(4\Delta e^{\bar{H}_t})$.

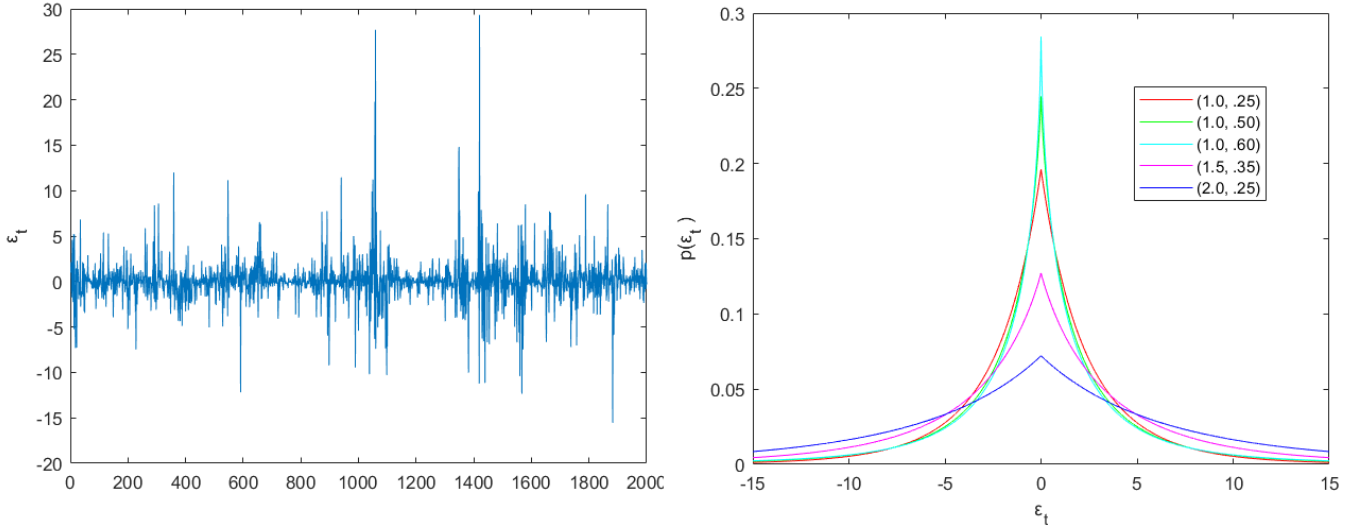


Figure 5: Left: A typical realization of the process ε_t defined in (1.1)-(1.4) with $z_t \sim \text{Lap}(0,1)$, $H_t = .5H_{t-1} + .4H_{t-2} + h_t$, and $\Delta = 1/4$. Right: Graphs of the probability density functions (B.3) with (\bar{H}_t, Δ) equal to (1, .25) in Red, (1, .50) in Green, (1, .60) in Cyan, (1.5, .35) in Magenta, and (2, .25) in Blue.

Then re-substituting for b_t and a_2 in the first term gives

$$\frac{1}{4\Delta} \exp\left(\frac{\bar{H}_t}{\Delta}\right) \Gamma\left(1 + \frac{1}{\Delta}\right) |\varepsilon_t|^{-1/\Delta-1}, \quad (\text{B.5})$$

which is the limit of (B.3)'s second term as $|\varepsilon_t| \rightarrow \infty$. Fully re-substituting in the second term and remainder term of (B.3)'s asymptotic expansion, applying the integral

$$\int_{\Lambda}^{\infty} e^{-\varepsilon/e^{\bar{H}_t}} \varepsilon^{-(k+1)} d\varepsilon = e^{-k\bar{H}_t} \Gamma\left(-k, \frac{\Lambda}{e^{\bar{H}_t}}\right), \quad (\text{B.6})$$

and cancelling factors then gives the result

$$\begin{aligned} P\{|\varepsilon_t| \geq \Lambda | \mathcal{F}_{t-1}\} &= \frac{1}{2} \Gamma\left(1 + \frac{1}{\Delta}\right) \exp\left(\frac{\bar{H}_t}{\Delta}\right) \Lambda^{-1/\Delta} \\ &+ \frac{1}{4\Delta} \sum_{k=1}^{n-1} \left[u_k \left(1 - \frac{1}{\Delta}\right) - u_k \left(1 + \frac{1}{\Delta}\right) \right] \Gamma\left(-k, \frac{\Lambda}{e^{\bar{H}_t}}\right) \\ &+ O\left(\Gamma\left(-n, \frac{\Lambda}{e^{\bar{H}_t}}\right)\right). \end{aligned} \quad (\text{B.7})$$

Then comparing (B.7) and (2.10) gives

$$P\{|\varepsilon_t| \geq \Lambda | \mathcal{F}_{t-1}\} \sim \Gamma\left(1 + \frac{1}{\Delta}\right) P\{\sigma_t \geq \Lambda | \mathcal{F}_{t-1}\}. \quad (\text{B.8})$$

Since $\Gamma(1) = \Gamma(2) = 1$, (B.8)'s second line reduces to $P\{|\varepsilon_t| \geq \Lambda | \mathcal{F}_{t-1}\} \sim P\{\sigma_t \geq \Lambda | \mathcal{F}_{t-1}\}$ for $\Delta = 1$ and as $\Delta \rightarrow \infty$. Several graphs of (B.3) are given in Fig. 5.

C Appendix 3: Non-Financial Empirical Applications

The stochastic volatility formalism described in Section 1-3 can be applied to non-financial time series as well. In this section we apply this modeling to two data sets respectively concerned with urban air pollution and solar activity. The first data set is the levels of PM2.5 particulate matter concentration (in $\mu g/m^3$) measured hourly at the U.S. Embassy in Beijing from January 1st, 2010 to December 31st, 2014 (see Liang et. al. 2015). A linear AR(44) model is fitted to the levels using the Yule-Walker method, with order selected using the Akaike Information Criterion (AIC). We then apply Section 1-3’s modeling to the AR(44) model’s corresponding residuals, using 41,665 samples over approximately 5 years. The second data set is monthly sunspot numbers observed from January, 1749 to July, 2014, retrieved from the Royal Observatory of Belgium. We similarly use Yule-Walker and AIC to fit a linear AR(29) model to the sunspot numbers. We then apply Section 1-3’s modeling to the AR(29) model’s corresponding residuals, using 3,124 samples over approximately 261 years. Hence for both applications we are using Section 1-3’s formalism to model the fluctuations in the data that are not captured by the linear autoregressive models.

We apply the same L1-penalized Principal Component Regression method for (3.3)’s \hat{H}_t as described in Section 5. However, we use $\{\hat{H}_{t-1}, \dots, \hat{H}_{t-48}\}$ for the Beijing PM2.5 data, giving its model for \hat{H}_t a memory length of 48 hours. For the sunspot data, we use $\{\hat{H}_{t-1}, \dots, \hat{H}_{t-24}\}$, giving its model for \hat{H}_t a memory length of 24 months. We again use (3.5)’s $\hat{\Delta} = \hat{\Delta}(4\hat{\sigma}_\varepsilon)$, and we study the volatility and dynamic probability estimates (5.4)-(5.5) as well as the binary classifier (5.7). Similarly to Section 5, we perform two sets of 100 backtests each for 50/50 and 60/40 train/test splits of the data sets. We give empirical results for $\hat{\Delta}(4\hat{\sigma}_\varepsilon)$, the correlation (5.6), and the sensitivity (5.8) and specificity (5.9) in Table 3.

We first note from Table 3 that the PM2.5 residuals are estimated to have much heavier tails than the SPX log-returns in Section 5, with $\hat{\Delta}$ estimated to be about .45. For the Beijing PM2.5 data, the classifier ξ_t exhibits sensitivity of 82% to 86%, which is accompanied by a specificity of about 66%. Additionally, the average correlation $\rho_{|\varepsilon|, \hat{\sigma}}$ is about 33%.

We next note from Table 3 that the sunspot residuals are estimated to have much lighter tails than the PM2.5 residuals, with $\hat{\Delta} \approx .20$. The sunspot data’s classifier ξ_t exhibits sensitivity of 84% to 92% and specificity of 65% to 70%. The average test correlation $\rho_{|\varepsilon|, \hat{\sigma}}$ is also about 33%.

These results show predictiveness on the test sets for both applications. However, we note that since the AR(44) and AR(29) models were calibrated over the entire data sets, there is potentially information from the test sets embedded within the training sets. Nevertheless, these applications show that Section 1-3’s methodology has great flexibility and can be useful for nonlinear, heavy-tailed time series modeling in many fields. Plots of the Beijing PM2.5 and sunspot data along with corresponding volatility and probability estimates are given in Fig. 6.

SUPPLEMENTARY MATERIAL

R scripts: R scripts containing code to perform the simulation studies in Section 4 and the empirical applications in Section 5 and Appendix 3. (.R files)

Data sets: Data sets used in the empirical applications in Section 5 and Appendix 3. (.xlsx files)

For supplementary materials email gordon.chavez@ucsf.edu.

Table 3: Non-Financial Application Results: Averages (\pm Standard Deviation)

Beijing PM2.5				
$N_{\text{Train}}/N_{\text{Test}}$	avg. $\widehat{\Delta}(4\widehat{\sigma}_\varepsilon)$	avg. $\rho_{ \varepsilon ,\widehat{\sigma}}$	avg. Sn.	avg. Sp.
20,833/20,832 (50/50)	.45 ($\pm .00$)	.34 ($\pm .00$)	.82 ($\pm .00$)	.68 ($\pm .00$)
24,999/16,666 (60/40)	.46 ($\pm .00$)	.33 ($\pm .00$)	.86 ($\pm .00$)	.65 ($\pm .01$)
Sunspots				
$N_{\text{Train}}/N_{\text{Test}}$	avg. $\widehat{\Delta}(4\widehat{\sigma}_\varepsilon)$	avg. $\rho_{ \varepsilon ,\widehat{\sigma}}$	avg. Sn.	avg. Sp.
1,562/1,562 (50/50)	.17 ($\pm .04$)	.33 ($\pm .01$)	.84 ($\pm .06$)	.70 ($\pm .02$)
1,874/1,250 (60/40)	.21 ($\pm .01$)	.34 ($\pm .00$)	.92 ($\pm .00$)	.65 ($\pm .01$)

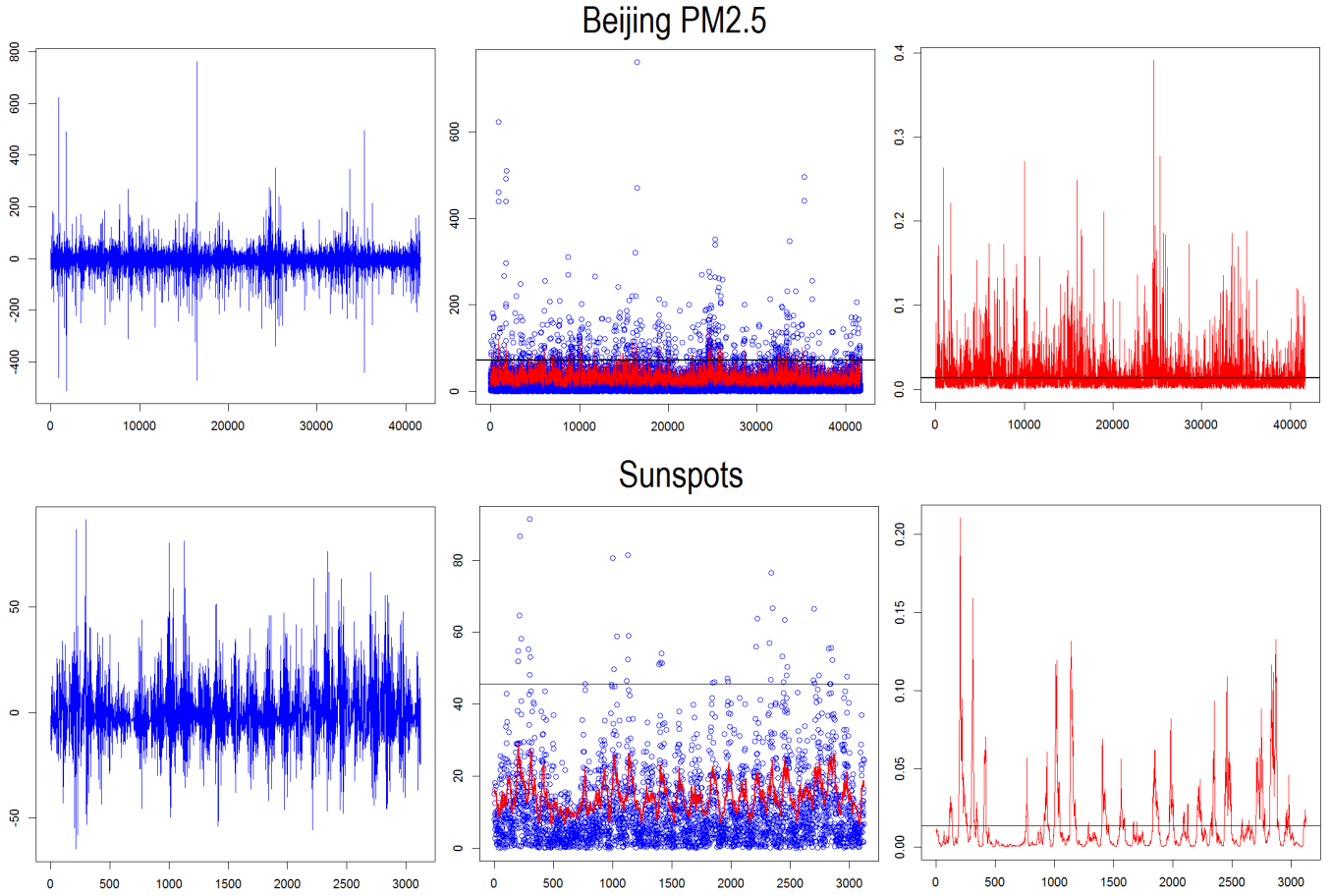


Figure 6: Top: Beijing PM2.5 Application. Bottom: Sunspots Application.

Left: Plots of the AR model residuals ε_t . Middle: Plots of $|\varepsilon_t|$ in Blue and (5.4)'s $\widehat{\sigma}_{\varepsilon,t}$ in Red with $3\widehat{\sigma}_\varepsilon$ marked in Black. Right: Plots of (5.5)'s $\widehat{P}\left\{|\varepsilon_t| \geq 3\widehat{\sigma}_\varepsilon | \widehat{H}_t, \widehat{\Delta}\right\}$ in Red with the threshold value for (5.7)'s ξ_t marked in Black. \widehat{H}_t is a sparse autoregressive model of order 48 (Top) and order 24 (Bottom), while $\widehat{\Delta}$ is given by (3.5)'s $\widehat{\Delta}(4\widehat{\sigma}_\varepsilon)$. The whole-sample results are $\widehat{\Delta}_{\text{Beijing PM2.5}} = .45$ and $\widehat{\Delta}_{\text{Sunspots}} = .20$.

References

- [1] Abramowitz, M. and I.A. Stegun (Editors) (1965). Handbook of Mathematical Functions. Dover. New York, NY.
- [2] Ardia, D. (2008). Financial Risk Management with Bayesian Estimation of GARCH Models. *Lecture Notes in Economics and Mathematical Systems 612*. Springer-Verlag. Berlin, Heidelberg.
- [3] Ardia, D. and L.F. Hoogerheide (2010). Bayesian estimation of the GARCH(1,1) model with Student-t innovations. *The R Journal* 2(2), 41-47.
- [4] Black, F. (1976). Studies of stock price volatility changes. *Proceedings of the 1976 Meetings of the American Statistical Association*, 171-181.
- [5] Board of Governors of the U.S. Federal Reserve System (2018). U.S. / Euro Foreign Exchange Rate retrieved from FRED, Federal Reserve Bank of St. Louis; <https://fred.stlouisfed.org/series/DEXUSEU>.
- [6] Bollerslev, T. (1986). Generalized autoregressive conditional heteroskedasticity. *Journal of Econometrics* 31(3), 307-327.
- [7] Bollerslev, T. and H.O. Mikkelsen (1996). Modeling and pricing long memory in stock market volatility. *Journal of Econometrics* 73(1), 151-184.
- [8] Breidt, F.J., N. Crato, and P. de Lima (1998). The detection and estimation of long memory in stochastic volatility. *Journal of Econometrics* 83(1-2), 325-348.
- [9] Chib, S., F. Nardari, and N. Shephard (2002). Markov chain Monte Carlo methods for stochastic volatility models. *Journal of Econometrics* 108(2), 281-316.
- [10] Chicago Board Options Exchange (2018). CBOE VIX Whitepaper: CBOE Volatility Index; <http://www.cboe.com/micro/vix/vixwhite.pdf>.
- [11] Christie, A.A. (1982). The stochastic behavior of common stock variances: value, leverage, and interest rate effects. *Journal of Financial Economics* 10(4), 407-432.
- [12] deHaan, L. and S.I. Resnick (1980). A simple asymptotic estimate for the index of a stable distribution. *Journal of the Royal Statistical Society Series B* 42(1), 83-87.
- [13] Diebold, F.X., T. Schuermann, and J.D. Stroughair (2000). Pitfalls and opportunities in use of extreme value theory in risk management. *Journal of Risk Finance* 1(2), 30-35.
- [14] Ding, Z., C.W.J. Granger, and R.F. Engle (1993). A long memory property of stock market returns and a new model. *Journal of Empirical Finance* 1(1), 83-106.
- [15] Embrechts, P., C. Kluppelberg, and T. Mikosch (2011). Modelling Extremal Events for Insurance and Finance. Springer. Heidelberg.
- [16] Engle, R.F. (1982). Autoregressive conditional heretoskedasticity with estimates of the variance of United Kingdom inflation. *Econometrica* 50(4), 987-1007.
- [17] Engle, R.F. and V.K. Ng (1993). Measuring and testing the impact of news on volatility. *Journal of Finance* 48(5), 1749-1778.

- [18] Fama, E.F. and R. Roll (1968). Some properties of symmetric stable distributions. *Journal of the American Statistical Association* 63(323), 817-836.
- [19] Friedman, J., T. Hastie, and R. Tibshirani (2010). Regularization paths for generalized linear models via coordinate descent. *Journal of Statistical Software* 33(1), 1-22.
- [20] Gardes, L. and S. Girard (2008). A moving window approach for nonparametric estimation of the conditional tail index. *Journal of Multivariate Analysis* 99(10), 2368-2388.
- [21] Gardes, L. and G. Stupfler (2014). Estimation of the conditional tail index using a smoothed local Hill estimator. *Extremes* 17(1), 45-75.
- [22] Grau-Carles, P. (2000). Empirical evidence of long-range correlations in stock returns. *Physica A: Statistical Mechanics and its Applications* 287(3-4), 396-404.
- [23] Harvey, A.C., E. Ruiz, and N. Shephard (1994). Multivariate stochastic variance models. *Review of Economic Studies* 61(2), 247-264.
- [24] Hill, B.M. (1975). A simple general approach to inference about the tail of a distribution. *Annals of Statistics* 3(5), 1163-1174.
- [25] Incomplete Gamma and Related Functions 8.11(i), Digital Library of Mathematical Functions, National Institutes of Standards and Technology; <https://dlmf.nist.gov/8.11>.
- [26] Jacquier, E., N.G. Polson, and P.E. Rosse (1994). Bayesian analysis of stochastic volatility models. *Journal of Business & Economic Statistics* 12(4), 371-389.
- [27] Jameson, G.J.O. (2016). The incomplete gamma functions. *The Mathematical Gazette* 100(548), 298-306.
- [28] Jameson, G.J.O. (2017). The incomplete gamma functions (notes); <https://www.maths.lancs.ac.uk/jameson/gammainc.pdf>.
- [29] Johnson, N.L., S. Kotz, and N. Balakrishnan (1994). Continuous Univariate Distributions Vol. 1. 14: Lognormal Distributions. Wiley. New York, NY.
- [30] Kearns, P. and A. Pagan (1997). Estimating the density tail index for financial time series. *The Review of Economics and Statistics* 79(2), 171-175.
- [31] Kelly, B. (2014) The dynamic power law model. *Extremes* 17(4), 557-583.
- [32] Kim, S., N. Shephard, and S. Chib (1998). Stochastic volatility: likelihood inference and comparison with ARCH models. *Review of Economic Studies* 65(3), 361-393.
- [33] Liang, X., T. Zou, B. Guo, S. Li, H. Zhang, S. Zhang, H. Huang, and S.X. Chen (2015). Assessing Beijing's PM2.5 pollution: severity, weather impact, APEC and winter heating. *Proceedings of the Royal Society A* 471(2182).
- [34] Liesenfeld, R. and R.C. Jung (2000). Stochastic volatility models: conditional normality versus heavy-tailed distributions. *Journal of Applied Econometrics* 15(2), 137-160.
- [35] Lobato, I.N. and N.E. Savin (1998). Real and spurious long-memory properties of stock-market data. *Journal of Business & Economic Statistics* 16(3), 261-268.

- [36] Mandelbrot, B.B. (1963). The variation of certain speculative prices. *Journal of Business* 36(4), 394-419.
- [37] McNeil, A.J. and R. Frey (2000). Estimation of tail-related risk measures for heteroscedastic financial time series: an extreme value approach. *Journal of Empirical Finance* 7(3-4), 271-300.
- [38] Mousazadeh, S. and M. Karimi (2007). Parameter estimation for Student-t ARCH model using MDL criterion. *2007 IEEE International Conference on Signal Processing and Communications*.
- [39] Nelson, D.B. (1991). Conditional heteroskedasticity in asset returns: a new approach. *Econometrica* 59(2), 347-370.
- [40] Pickands, J. (1975). Statistical inference using extreme order statistics. *Annals of Statistics* 3(1), 119-131.
- [41] Ray, B.K. and R.S. Tsay (2000). Long-range dependence in daily stock volatilities. *Journal of Business & Economic Statistics* 18(2), 254-262.
- [42] Rohatgi, V.K. (1976). An Introduction to Probability Theory and Mathematical Statistics. Wiley. New York, NY.
- [43] Sandmann, G. and S.J. Koopman (1998). Estimation of stochastic volatility models via Monte Carlo maximum likelihood. *Journal of Econometrics* 87(2), 271-301.
- [44] Taylor, S.J. (1982). Financial returns modelled by the product of two stochastic processes—a study of daily sugar prices 1961-1979. In Anderson, O.D. (Editor), *Time Series Analysis: Theory and Practice*, Vol. 1. Amsterdam, North-Holland. 203-226.
- [45] Taylor, S.J. (1986). *Modeling Financial Time Series*. Wiley. Chichester.
- [46] Terasvirta, T., D. Tjøstheim, and C.W.J. Granger (2010). *Modelling Nonlinear Economic Time Series*. Oxford. New York.
- [47] Tibshirani, R. (1996). Regression shrinkage and selection via the Lasso. *Journal of the Royal Statistical Society. Series B* 58(1), 267-288.
- [48] WDC-SILSO, Solar Influences Data Analysis Center (SIDC), Royal Observatory of Belgium, Av. Circulaire, 3, B-1180 BRUSSELS; <http://www.sidc.be/silso/datafiles>.